International Journal of Mechanics and Energy (IJME)
Vol. 1, Issue 4, 2013, ISSN: 2286-5845

Numerical investigation of natural convection of CuO-water nanofluid

Mefteh Bouhalleb, Hassan Abbassi
Unit of Computational Fluid Dynamics and Transfer Phenomena,
National Engineering School of Sfax. University of Sfax, TUNISIA
Corresponding author: meftehbouhalleb@gmail.com

Abstract: This paper analyzes heat transfer and fluid flow of natural convection in an inclined cavity filled with CuO/water nanofluid that operates under differentially heated walls. The transport equations for the flow are solved numerically by the finite volume element method using the SIMPLER algorithm. Simulations are performed for various aspect ratios. The inclination angle is varied between 0 and 90°, and the Rayleigh number is in the range of 10^3 and 10^5. Temperature distribution and heat transfer rates are analyzed and discussed. It is found that the addition of solid nanoparticles in working fluid lead to a considerable enhancement of heat transfer. Effects of aspect ratio, inclination angle, and Rayleigh number on heat transfer are analyzed.

Key words: Nanofluid, Natural convection, Heat transfer, Solid volume fraction

1. Introduction

The fluids that are traditionally used for heat transfer applications such as water, mineral oils and ethylene glycol have a rather low thermal conductivity. Such classic fluids present a limitation in enhancing the heat transfer performance. Scientists and engineers have started showing interest in the study of heat transfer characteristics of nanofluids which are pure fluid with some additional solid nanoparticles. Over the last years, it has been demonstrated that thermal conductivity of fluids suspended with metallic nanoparticles is significantly higher than that of pure fluids. Kim et al.[1] investigated analytically the instability in natural convection of nanofluids. They proposed a new factor that describes the effect of nanoparticles addition on the convective instability and heat transfer characteristics of a base fluid. Their results show that, as the density and heat capacity of nanoparticles increase and the thermal conductivity and shape factor of nanoparticles decrease, the convective motion of a nanofluid sets in easily. All the experimental results have demonstrated the enhancement of the thermal conductivity by the addition of nanoparticles. Eastman et al.[2] used pure copper nanoparticles of less than 10 nm, they obtained 40% increase in thermal conductivity for only 0.3% volume fraction of the solid dispersed in ethylene glycol. Parvin et al.[3] analyzed thermal conductivity variation on natural convection flow of water–alumina nanofluid in an annulus. They observed significant heat transfer enhancement due to the presence of nanoparticles and it was accentuated by the increasing of the nanoparticles volume fraction and Prandtl number as well as large Grashof number. Control volume finite element simulation of MHD forced and natural convection in a vertical channel with a heat-generating pipe was analyzed by Nasrin and Alim [4]. This study addresses the effects of nanoparticles volume fraction, Rayleigh number, inclination angle and aspect ratio on CuO/water nanofluid to simulate natural convection in a rectangular enclosure.

The theatrical prediction in this paper is hoped to be a useful guide for the experimentalists to study the effectiveness of the natural convection in a rectangular enclosures filled with CuO/water nanofluids to increase rate of heat transfer.

2. Statement of the problem

In this study, we consider a rectangular cavity of length L and height H as shown in figure 1. The cavity is filled with water-CuO and its bottom and top walls are respectively maintained at high and cold temperature. The nanofluid is supposed to be Newtonian and incompressible; the flow is laminar and two-dimensional. The base fluid (water) and the spherical nanoparticles (CuO) are supposed to be in thermal equilibrium. The thermo physical properties of the base fluid and the solid particles are given in Table 1. The thermo physical properties of the nanofluid are assumed constant except for the density variation, which is determined on the basis of on the Boussinesq approximation.

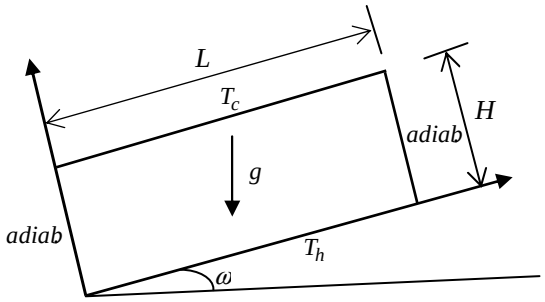

Fig. 1 differentially heated cavity

Table 1 Physical properties of pure water and CuO

	ρ (kg.m^{-3})	C_p (J.kg^{-1}.K^{-1})	k (W.m^{-1}.K^{-1})	β (k^{-1})
Pure water	997.1	4179	0.613	2.1×10^{-4}
CuO	6320	531.8	76.5	1.8×10^{-5}

3. Mathematical formulation

Equations are formulated considering the usual hypotheses of a newtonian incompressible fluid under the Boussinesq approximation. In the Cartesian coordinate system, the dimensionless equations for continuity momentum and energy may be expressed in the following form:

$$\frac{\partial u}{\partial x}+\frac{\partial v}{\partial y}=0 \quad (1)$$

$$u\frac{\partial u}{\partial x}+v\frac{\partial u}{\partial y}=-\frac{\partial p}{\partial x}+\frac{\mu_{nf}}{\rho_{nf}\alpha_f}\left(\frac{\partial^2 u}{\partial x^2}+\frac{\partial^2 u}{\partial y^2}\right)+\frac{(\rho\beta)_{nf}}{\rho_{nf}\beta_f}Ra\,\Pr\theta\sin\omega \quad (2)$$

$$u\frac{\partial v}{\partial x}+v\frac{\partial v}{\partial y}=-\frac{\partial p}{\partial y}+\frac{\mu_{nf}}{\rho_{nf}\alpha_f}\left(\frac{\partial^2 v}{\partial x^2}+\frac{\partial^2 v}{\partial y^2}\right)+\frac{(\rho\beta)_{nf}}{\rho_{nf}\beta_f}Ra\,\Pr\theta\cos\omega \quad (3)$$

$$u\frac{\partial \theta}{\partial x}+v\frac{\partial \theta}{\partial y}=\frac{\alpha_{nf}}{\alpha_f}\left(\frac{\partial^2 \theta}{\partial x^2}+\frac{\partial^2 \theta}{\partial y^2}\right) \quad (4)$$

Equations (1)-(4) are normalized by the characteristic length L of the cavity and specific velocity α/L where α is the thermal diffusivity of the fluid. The dimensionless temperature θ is defined as $\theta=(T-T_c)/(T_h-T_c)$.

The expressions of density, specific heat, thermal expansion coefficient and dynamic viscosity all of the nanofluid are given as follows:

$$\rho_{nf}=(1-\varphi)\rho_f+\varphi\rho_s \quad (5)$$

$$(\rho C_p)_{nf}=(1-\varphi)(\rho C_p)_f+\varphi(\rho C_p)_s \quad (6)$$

$$(\rho\beta)_{nf}=(1-\varphi)(\rho\beta)_f+\varphi(\rho\beta)_s \quad (7)$$

$$\mu_{nf}=\frac{\mu_f}{(1-\varphi)^{2.5}} \quad (8)$$

The local Nusselt number *Nu(x)* can is expressed as:

$$Nu(x)=-\frac{k_{eff}}{k_f}\left(\frac{\partial\theta}{\partial y}\right)_{y=0} \quad (9)$$

Effective conductivity k_{eff} of the nanofluid is calculated as follows [5]:

$$k_{eff}=k_{stat}+k_{brow} \quad (10)$$

The static conductivity k_{stat} is given by the Maxwell model [5] as:

$$k_{stat} = k_f \frac{k_S + 2k_f + 2(k_S - k_f)\varphi}{k_S + 2k_f - (k_S - k_f)\varphi} \qquad (11)$$

The brownian conductivity is formulated as (Koo and Kleinstreuer [6]):

$$k_{brow} = 5\times10^4 \beta_1 \varphi (\rho C_p)_f \sqrt{\frac{\kappa T}{\rho_S D_S}} f(T,\varphi) \quad (12)$$

Where ρ_s and D_s are the density and the diameter of solid nanoparticles, respectively and κ is the Boltzmann constant κ=1.3807x10^{-23}J/K. For the water-CuO nanofluid, the two modeling functions β_1 and f are experimentally estimated as:

$$\beta_1 = 0.0011(100\phi)^{-0.7272}$$

$$f(T,\phi) = (-6.04\phi + 0.4705)T + (1722.3\phi - 134.63)$$

These expressions are valid for 1%≤ϕ≤4%**.**

The total heat transferred from the hot wall to the flow is evaluated by the space averaged Nusselt number expressed as:

$$Nu = \frac{1}{Ar}\int_0^{Ar} Nu(x)dx \qquad (13)$$

4. Numerical methodology

A modified version of Control Volume Finite-Element Method (CVFEM) is adapted to the standard staggered grid in which pressure and velocity components are stored at different points. The SIMPLER algorithm of Patankar was applied to resolve the pressure-velocity coupling in conjunction with an Alternating Direction Implicit (ADI) scheme for performing the time evolution.

5. Grid refinement and test validation

Grid refinement tests have been performed for four grids: 41×41, 51×51, 61×61 and 71×71 for Ra=10^5, φ=0.04 and ω=0°. Results show that when we passes from the first grid to the second, the Nusselt number Nu passes from 4.6634 to 4.6535, undergoing a variation of 0.2%. When we pass from the second grid to the third, the Nusselt number becomes 4.6468, undergoing a decrease of 0.14%. Now when we pass from the third grid to the fourth, the Nusselt number becomes 4.6431, undergoing a decrease of only 0.07%. We conclude that the grid of 61×61 ensures the independence of the numerical results from the grid size.

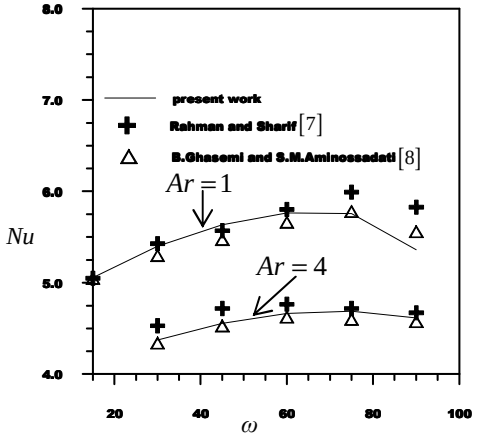

Fig. 2 Test validation

The validation of the present computer code for natural convection in an inclined enclosure was assessed. This assessment was carried out by comparing the results with the study by Rahman and Sharif [7] and Ghasemi and Aminossadati [8]. Figure 2 shows the variation of Nu along the hot wall with inclination angle at two different aspect ratios Ar. A reasonable agreement can be observed between obtained results and the above references.

6. Results and discussions

Numerical simulations are performed for CuO-water as working fluid with Prandt number of 7.06. The aspect ratio Ar is considered for four different values 0.5, 1, 2 and 4. The solid volume fraction is varied in the range 0%-8%; Rayleigh numbers and inclination angle are ranging from 10^3 to 10^5 and 0° to 90°respectively.

Streamlines and isotherms for different aspect ratios are presented in figures 3 – 6 for a constant concentration ϕ=0.04 at Rayleigh number Ra=10^5.

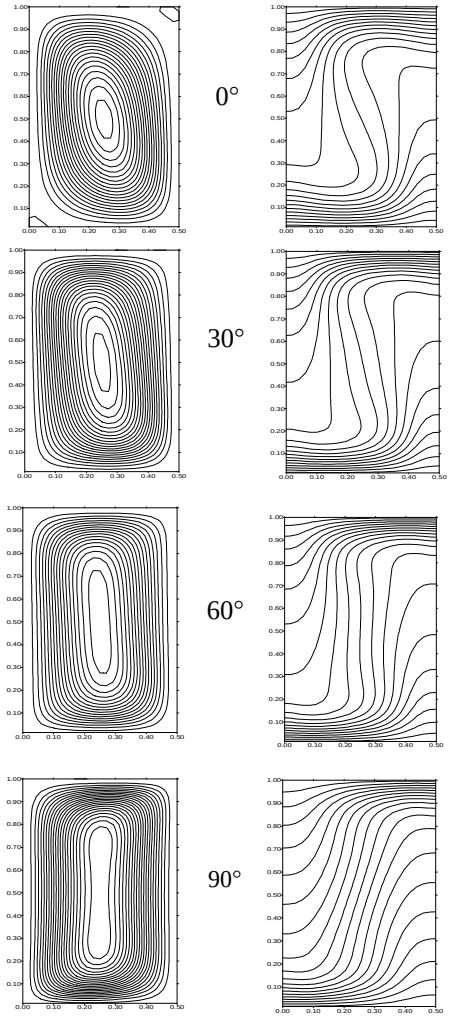

Fig.3 Streamlines and isotherms (Ra=10^5, ϕ =0.04, Ar=0.5)

For the configuration of Ar=0.5, the flow is characterized by the apparition of simple cell circulating in an anticlockwise for all inclination angles. The increasing of inclination angle makes the circulation cell become elliptic but the flow remains unicellular. For the aspect ratio Ar=1, when the cavity is placed horizontally; that is to say the angle of inclination is equal to 0, the flow is characterized by the apparition of two cells turning in opposite sense inside the cavity. The fluid rises from the middle of the hot wall towards the cold upper wall and descends on sides of the enclosure. Once we increase the inclination angle to reach 7°, the last flow is destabilized; the two cells disappear and a single cell flow takes place. The fluid rises from the right down side wall and forms a single circulation cell rotating in the anticlockwise sense. When, the inclination angle increases, the cell becomes more elliptical.

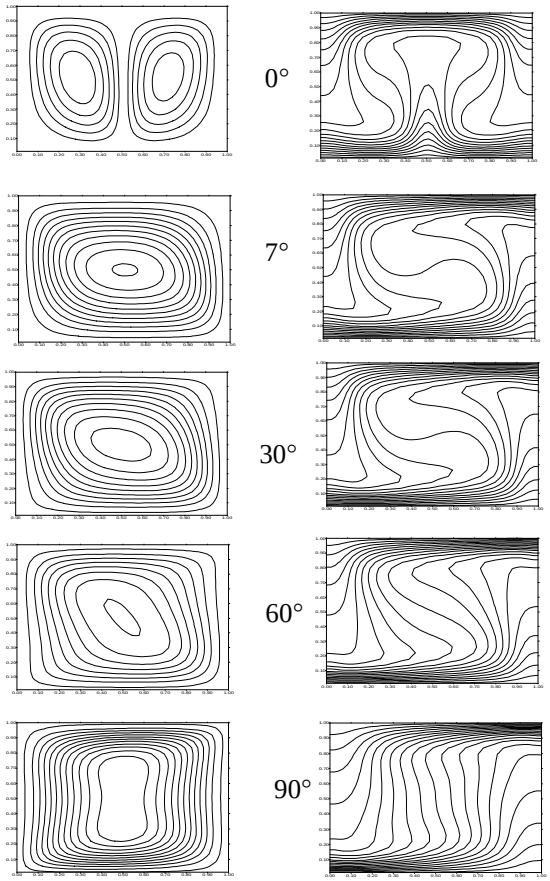

Fig.4 Streamlines and isotherms for different inclination angles (Ra=10^5, φ=0.04, Ar=1.0)

Regarding to isotherms for Ar=1, at ω=0 there is been a rather symmetrical pattern within the enclosure, when ω increases so that the flow becomes unicellular, this symmetry is lost, near the working

walls, isotherms tend to become parallel to these walls at the central cavity.

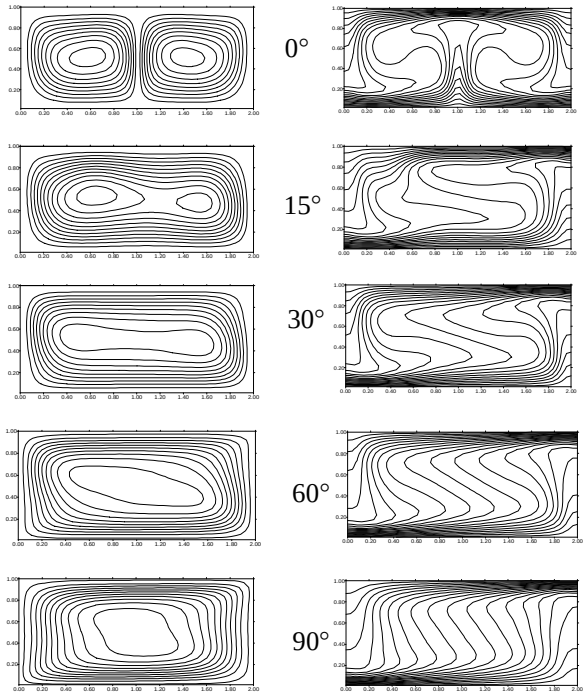

Fig. 5 Streamlines and isotherms for different inclination angles ($Ra=10^5$, $\phi=0.04$, $Ar=2$)

In the case $Ar=2$, when $\omega=0$, streamlines show that there are two symmetric cells about the vertical mid-plane of the cavity, turning in opposite sense inside the cavity. Increasing slowly the inclination angle, the last flow is destabilized and the upper cell decrease in size whereas the down one increases in size. When ω exceeds 30° a single cell rotating in the anticlockwise sense takes place. Concerning isotherms, when ω=0°, the temperature gradients near both the heated and the cooled walls start to be thick enough to suggest the development of thermal boundary layers. When ω increases so that the flow becomes of single cell, the isotherms tend to become parallel to the adiabatic walls at the central cavity.

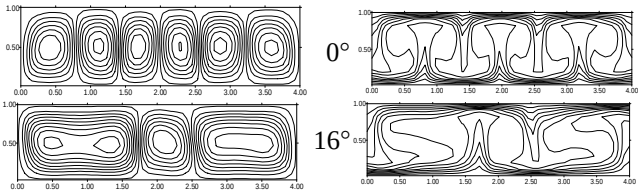

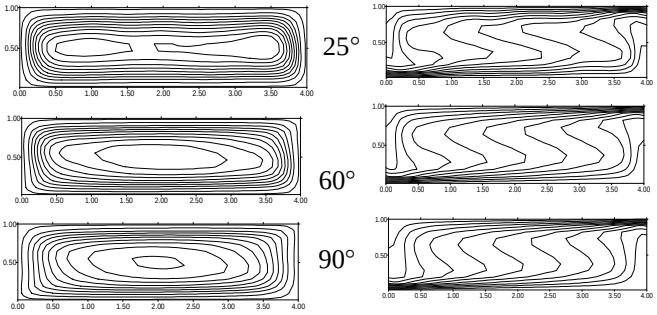

Fig. 6 Streamlines and isotherms for different inclination angles ($Ra=10^5$, $\phi=0.04$, $Ar=4$)

For $Ar=4$, at $\omega=0°$ a six-cell flow pattern is observed. Increasing the inclination angle ω slowly, when reaching 16°, transition in flow pattern is observed. The number of cells is reduced to only three. Further increasing the inclination angle, the whole cavity was occupied by one cell rotating in the anticlockwise sense.

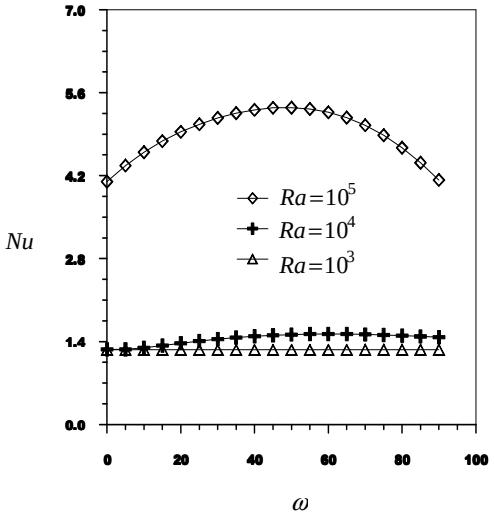

Fig. 7 Average Nusselt number at various inclination angles for $Ar=0.5$ and $\phi=0.04$

Fig. 7 shows average Nusselt number, at different Rayleigh numbers, as a function of inclination angle. For low Rayleigh numbers ($Ra\leq10^4$), numerical simulations show no significant variation in *Nu*. The low value in *Nu* (slightly greater than 1 which corresponds to pure conduction), show that heat transfer is made essentially by conduction mode, convection mode is still insignificant. For high

Rayleigh numbers, *Nu* increases considerably; it increases with increasing ω, reaches a maximum and decreases. This maximum is obtained at ω=45°. The unicellular flow pattern observed for all cavity position (i.e., ω=0° to 90°) for *Ar*=0.5, make no sudden variation in *Nu*.

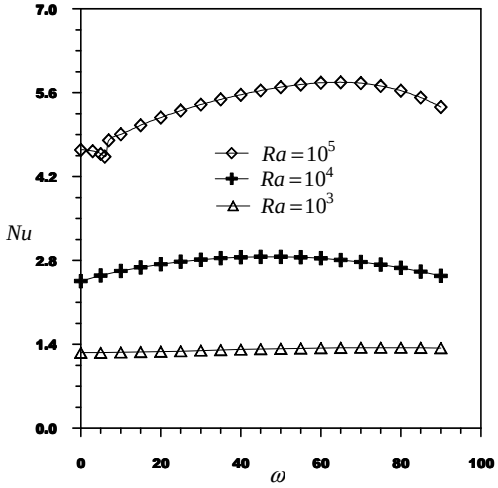

Fig. 8 Average Nusselt number at various inclination angles for *Ar*=1. and ϕ=0.04

Figure 8 shows average Nusselt number at various Rayleigh numbers as a function of inclination angle for *Ar* =1. At ω=0°, a two-cell flow pattern was observed. As ω increased slightly above 7°, the upslope temperature gradient cause a change in the number of cells from two to one, which resulted in a slight drop in Nusselt number as shown in figure 8 at $Ra=10^5$. At weak Rayleigh numbers, this sudden drop is not observed; this is due to the presence of a one cell flow and then no change in flow structure when varying ω.

In the case *Ar*=2 (fig.9), at low Rayleigh numbers such as $Ra=10^3$, the variation of *Nu* with ω is not significant, the heat is still transferred by conduction mode and then the orientation of the cavity has no significant effects. For high Rayleigh numbers, *Nu* started by a decrease, reaches a minimum and increases until a maximum value. The decay phase is due to the change in flow pattern, the decrease in size of the upper cell until its disappearance is at the origin of the decrease in heat transfer. For $Ra=10^5$, the maximum value of *Nu* is reached at ω=65°.

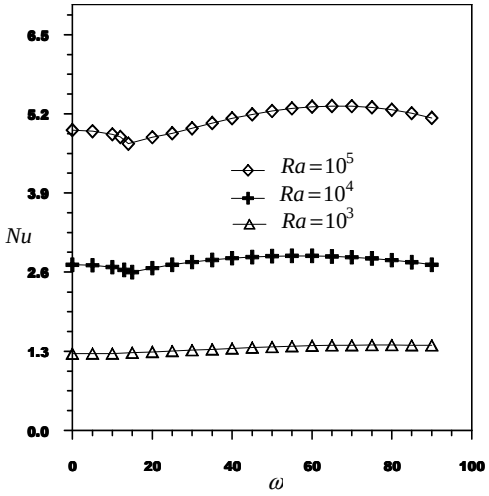

Fig. 9 Average Nusselt number as a function of inclination angles for *Ar*=2.0 and ϕ=0.04

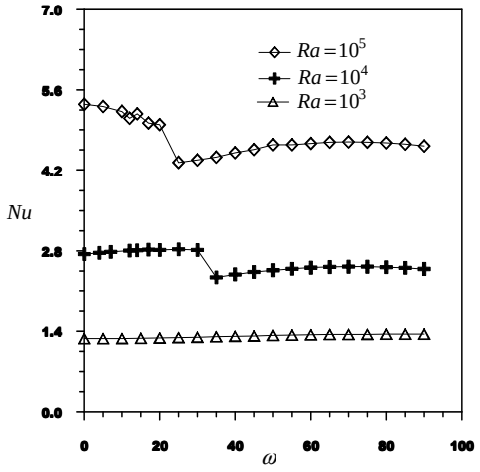

Fig. 10 Average Nusselt number at various inclination angles for *Ar*=4.0 and ϕ=0.04

For *Ar*=4, figure 10 confirm that for low Rayleigh numbers, no significant effects of cavity orientation on heat transfer; conduction is the dominating mode. For higher Rayleigh numbers, as *Ra* increased, a noticeable drop in Nusselt number appears. This change in the rate of heat transfer is in direct relation of the mode-transition of the flow pattern. Figure 10 also indicates that the angle at which mode transition takes place depends on the value of Rayleigh number. As *Ra* decreased, mode-transition was delayed, i.e.,

take place at a larger angle of inclination. Numerical simulations show that the mode transition in *Nu* is happened at inclination angles 25° and 16° for $Ra=10^4$ and 10^5 respectively. This transition caused a sudden drop in average Nusselt number.

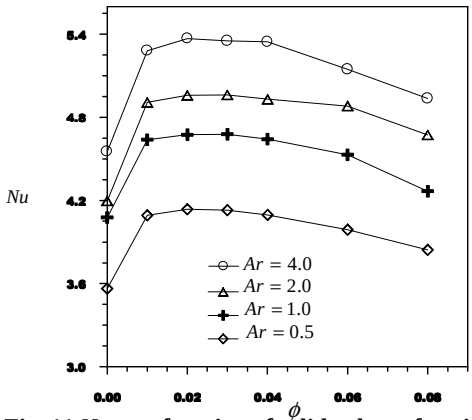

Fig. 11 *Nu* as a function of solid volume fraction ϕ

$Ra=10^5$, $\omega=0°$

The average Nusselt number along the hot wall as a function of solid volume fraction is shown in figure 11. For all aspect ratios, increasing, the solid volume fractionϕ in the nanofluid increases *Nu* until a maximum and decreases. The maximum of Nu is recorder at ϕ=2% where brawnian effects plays a role in increasing the thermal conductivity of the working fluid as mentioned in equation (12). This result confirms that the addition of nanosolid of high thermal conductivity to the basic fluid leads to heat transfer enhancement via the augmentation of the thermal conductivity of the working fluid. Figure 11 show also that heat transfer increases considerably with increasing the aspect ratio. The addition of nanosolid above 2% lead to a decrease in heat transfer and the situation becomes out of practical interest.

7. Conclusion

In this study, the laminar incompressible flow of CuO-water in a rectangular enclosure submitted to vertical temperature gradient is simulated. The coupled non linear equations of momentum and energy including buoyancy forces under the Boussinesq approximation are solved numerically using the finite volume. Based on the finding results, we can get the fallowing conclusions.

1. The addition of nanosolid particle into the working fluid leads to a considerable enhancement of heat transfer. A concentration of 2% provides a maximum heat transfer.
2. The variation of inclination angle lead to a considerable change in flow pattern. For *Ar*=1, 2 and 4, the increase in inclination angle causes the transition from multi-cell flow to uni-cell. This transition is accompanied by a sudden drop in Nusselt number
3. At low Rayleigh numbers, heat transfer is achieved essentially by conduction mode, and then the cavity orientation has no effects on heat transfer, whereas at high to moderate *Ra* values, an optimum inclination angle is recorded.

References

[1] J. Kim, Y. T. Kang, C.K. Choi, Analysis of convection instability and heat transfer characteristics of nanofluids, *Phys Fluids* 2004;16:2395–401

[2]J. A. Eastman, S. Choi, S. Li, W. Yu, L. J. Thompson, Anomalously increased effective thermal conductivities of ethylene glycol-based nanofluids containing copper nanoparticles, *Appl Phys Lett* 2001;78:718–20.

[3] S. Parvin, R. Nasrin, M.A. Alim, N.F. Hossain, A.J. Chamkha, Thermal conductivity variation on natural convection flow of water–alumina nanofluid in an annulus, *Int. J. Heat Mass Transfer* 55 (2012) 5268–5274.

[4] R. Nasrin, M.A. Alim, Control volume finite element simulation of MHD forced and natural convection in a vertical channel with a heat-generating pipe, *Int. J. Heat Mass Transfer 55* (2012) 2813–2821.

[5] J. Maxwell, A Treatise on Electricity and Magnetism, 2nd ed., pp. 435–441, Oxford University Press, Cambridge, UK, 1904.

[6] J. Koo and C. Kleinstreuer, A New Thermal Conductivity Model for Nanofluids, *J. Nanoparticle Res.*, vol. 6, pp. 577–588, 2004.

[7] M. Rahman and M. A. R. Sharif, Numerical Study of Laminar Natural Convection in Inclined Rectangular Enclosures of Various Aspect Ratios, Numer. Heat Transfer, part A, vol. 44, pp. 355–373, 2003.

[8] B.Ghasmi and S.M.Aminossadati, natural convection heat transfer in an inclined enclosure filled with a water-CuO nanofluid, numerical heat transfer, part A, 55: 807-823,2009.

.